



Université Scientifique et Médicale de Grenoble

INSTITUT DES SCIENCES NUCLÉAIRES  
DE GRENOBLE

53, avenue des Martyrs - GRENOBLE

ISN 81.18  
April 1981HIGH-SPIN STATES IN  $^{60}\text{Cu}$ TSAN UNG CHAN, M. AGARD<sup>1</sup>, J.F. BRUANDET, B. CHAMSON<sup>2</sup>,  
A. DAUCHY, D. DRAIN<sup>2</sup>, A. GIORNI, F. GLASSER, C. MORAND<sup>1</sup>*Institut des Sciences Exactes, Université de Constantine (Algérie)*<sup>2</sup>*Institut de Physique Nucléaire de Lyon.*

HIGH-SPIN STATES IN  $^{60}\text{Cu}$

Tsan Ung Chan, M. Agard<sup>1</sup>, J.F. Bruandet, B. Chambon<sup>2</sup>, A. Dauchy, D. Drain<sup>2</sup>,

A. Giorni, F. Glasser and C. Morand

ABSTRACT.- The  $^{60}\text{Cu}$  nucleus has been studied via the  $^{58}\text{Ni}(\alpha, p\gamma)$  reaction using different in-beam  $\gamma$  spectroscopy techniques. As for the other odd-odd Cu, the  $g_{9/2}$  shell plays an important role for the explanation of observed high-spin states. Some of them (in particular  $6^-$  and  $9^+$  states) could be interpreted as two-nucleon states in the framework of a crude shell model.

NUCLEAR REACTIONS  $^{58}\text{Ni}(\alpha, p\gamma)$  E = 23-40 MeV, measured  $\sigma(E, E_\gamma, \theta)$ ,  $\gamma\gamma$ -coinc.,  $\gamma(t)$ ,  $^{60}\text{Cu}$  deduced levels, J,  $\pi$ ,  $\gamma$ -branching. Isotopic target.

1) Institut des Sciences Exactes, Université de Constantine, Route d'Ain El Bey  
Constantine, Algérie.

2) Institut de Physique Nucléaire (UCB Lyon, IN2P3), 43, Bd. du 11 Novembre,  
69621 Villeurbanne, France.

1) Introduction

The  $(\alpha, d)$  (Ref.1) and the  $(\alpha, {}^2\text{He})$  (Ref.2) reactions are known to be very selective. They populate preferentially two-nucleon high-spin states where the two transferred nucleons are coupled to their maximum spin value. We have deduced a very simple rule <sup>3)</sup> from the crudest shell-model picture : the energy of such a two-nucleon state is simply equal to the sum of the two individual single-particle energies plus a pairing energy when the two nucleons are identical. This simple calculation without any free parameter could account for a large number of experimental data involving two-nucleon states populated by the  $(\alpha, d)$  reaction or the  $(\alpha, {}^2\text{He})$  reaction.

We have shown in the study of  ${}^{62}\text{Cu}$  and  ${}^{64}\text{Cu}$  (ref. 3,4,5) that some high spin states (often yrast states) excited through  $(\alpha, pny)$  fusion evaporation reactions can be identified to strongly excited ones in the  $(\alpha, d)$  reaction. These two-nucleon states probably have rather pure configurations :  $(\pi f_{5/2}, \nu f_{5/2})_5^+$ ,  $(\pi p_{3/2}, \nu g_{9/2})_6^-$ ,  $(\pi g_{9/2}, \nu p_{3/2})_6^-$ ,  $(\pi f_{5/2}, \nu g_{9/2})_7^-$ ,  $(\pi g_{9/2}, \nu f_{5/2})_7^-$  and  $(\pi g_{9/2}, \nu g_{9/2})_9^+$ .

The present work on  ${}^{60}\text{Cu}$  is part of a systematic study of high-spin states in odd-odd copper and preliminary results have been presented at the Conference of Hvar <sup>6)</sup>.

All the available informations through April 1979 about  ${}^{60}\text{Cu}$  have been summarized by Auble <sup>7)</sup>. Only a few levels with low energy excitation are well known. Recently, Zimmerman et al <sup>8)</sup> have determined by the  $({}^3\text{He}, t)$  reaction many levels in  ${}^{60}\text{Cu}$  with a precision of  $\pm 10$  keV. However,  $J^\pi$  values are not unique. The  $\gamma$  decay scheme of  ${}^{60}\text{Cu}$  is deduced mainly from the radioactivity of  ${}^{60}\text{Zn}$  (ref.9) and from the  ${}^{60}\text{Ni} (p, ny) {}^{60}\text{Cu}$  (Ref. 10) reaction. Hoffman et al. <sup>10)</sup> have proposed a level scheme of  ${}^{60}\text{Cu}$  from the  ${}^{58}\text{Ni} (\alpha, pny) {}^{60}\text{Cu}$  reaction at  $E_\alpha = 22$  MeV up to only 700 keV because of the high Q value ( $Q = - 14.8$  MeV) of this reaction. We use here the same reaction but with  $\alpha$  of 32 MeV feeding then the high-spin states lying at a greater excitation energy.

## 2. EXPERIMENTAL PROCEDURE

Using beams from the Grenoble cyclotron, isotopic  $\sim 1 \text{ mg/cm}^2$   $^{58}\text{Ni}$  targets, large volume Ge(Li) detectors ( $50\text{-}90 \text{ cm}^3$ ) with a typical resolution of 3 keV at  $E_\gamma = 1.3 \text{ MeV}$ , the following measurements have been undertaken :

- yield functions of  $\gamma$ -rays :  $E_\alpha = 23 - 40 \text{ MeV}$
- angular distributions at  $E_\alpha = 32 \text{ MeV}$
- $\gamma$ - $\gamma$  coincidences at  $E_\alpha = 32 \text{ MeV}$
- lifetimes measurements with DSAM at  $E_\alpha = 32 \text{ MeV}$

Fig. 1 shows a single  $\gamma$ -ray spectrum of  $^{58}\text{Ni} + \alpha$  at  $E_\alpha = 32 \text{ MeV}$ . The main channels are  $(\alpha, 2p\gamma)^{60}\text{Ni}$ ,  $(\alpha, p\gamma)^{60}\text{Cu}$  and  $(\alpha, ap\gamma)^{57}\text{Co}$  with a relative intensity of 6, 3, 1. A precise calibration of high energy gamma rays are furnished by intense gamma rays from the radioactivity of  $^{60}\text{Co}$  (particularly we used the following  $\gamma$  rays : 1332.5, 1791.6, 2158.9 and 3124.1 keV).

## 3. ANALYSIS OF DATA :

3.1. Yield functions : They have been measured at 23, 27, 32, 36 and 40 MeV. Fig. 2 shows the relative intensity of some  $\gamma$  rays. We noticed that, as for other  $(\alpha, p\gamma)$  reactions with Ni targets, they are flat except for  $\gamma$  issued from high-spin states.

3.2. Angular distributions : They have been performed at 8 angles from  $30^\circ$  to  $150^\circ$ , on an isotopic target with Bi backing to reduce Doppler shifts. Results of the analysis are gathered in Table 1. We use formula and sign convention of Yamazaki <sup>12</sup>).

3.3.  $\gamma\gamma$  coincidences : An electronic timing measurement has shown no isomeric levels with  $T_{1/2} > 2 \text{ ns}$ . Thus, prompt  $\gamma\gamma$  coincidences are sufficient to establish the level scheme. The data are recorded on magnetic tapes in the 2048 x 2048 format ( $E_\gamma$  up to 2 MeV with one GeLi and up to 4 MeV in the other GeLi). The two GeLi detectors were perpendicular to the beam axis.

The angle between them was  $90^\circ$  and they were separated by a thick sheet of Pb : in this way, the 511-511 keV coincidence from  $\beta^+$  decay of  $^{60}\text{Cu}$  and the back scattering from one detector to the other are strongly reduced. Fig.3 presents some selected spectra observed in coincidence with events in the indicated gate regions and with subtracted backgrounds.

### 3.4. DSAM LIFETIME MEASUREMENTS

3.4.1. Measurements with a self supporting target : the method broadly exposed in ref. 13 uses the fact that the target is self supporting ( $0.9 \text{ mg/cm}^2$  thickness). A  $\gamma$  transition of long lifetime is used (here the 1084 keV transition in  $^{60}\text{Ni}$  with a lifetime of  $\tau = 423 \pm 70 \text{ ps}$  after the work of Moyat et al<sup>14</sup>) to determine the nuclear stopping power which is assumed to have the following form :  $\frac{dE}{dP} = ax/\exp(\frac{1}{2}x^2)$  with  $x = b z^{1/2}$ . The values of a and b are  $a = 0.77$  and  $b = 1.1$ . They are about the same as the values used in other  $\alpha + \text{Ni}$  or  $\alpha + \text{Zn}$  reactions. Results of lifetime measurements are presented in Table 2.

3.4.2. Rough estimations of lifetimes from spectra obtained on a target with Bi backing : From the view point of DSAM, the prompt  $\gamma$  rays ( $T_{1/2} < 2\text{ns}$ ) limit of electronic timing method for a self supporting target may be divided into two categories :

- i) "long lifetimes"  $\gamma$  rays ( $\tau > 4\text{ps}$ ) where the Doppler shift is mainly due to emitting nuclei going out from the  $0.9 \text{ mg/cm}^2$  target
- ii) "short lifetime"  $\gamma$  rays with  $\tau < 0.6 \text{ ps}$  : the observed Doppler shift is due essentially to  $\gamma$  from nuclei recoiling inside the target. This upper limit is provided by the stopping time of a  $^{60}\text{Ni}$  or  $^{60}\text{Cu}$  recoiling with an initial velocity of  $\beta = 0.85\%$  (the center of mass velocity). The dispersion of velocity introduced by evaporated particles leads to increase the upper limit of the ii) category to 2 ps and to decrease the lower limit of the i) category to 1 ps-.

The effect of a Bi backing is quite different for these two classes of  $\gamma$ . For the i) category because of the large stopping power of Bi, the recoiling nucleus is rapidly stopped so the Doppler shift is suppressed. The corresponding  $\gamma$  peak is about the same at any angle. On the contrary Bi backing has no effect on  $\gamma$  of the ii) category

This difference of behaviour is illustrated in Fig. 4 which presents prompt  $\gamma$  spectra at  $40^\circ$ ,  $90^\circ$  and  $160^\circ$ . It can be verified that the  $\gamma$  rays of  $^{60}\text{Cu}$  (except the 1640 keV one) and the  $\gamma$  of 1084 keV in  $^{60}\text{Ni}$  ( $\tau = 420$  ps) belong to the i) category. On the contrary, most of the  $\gamma$  rays in  $^{57}\text{Co}$  (Ref. 15) and a few  $\gamma$  of the Yrast line of  $^{60}\text{Ni}$  (Ref. 14) with short lifetimes belong effectively to the ii) category. We notice also that the 2291 keV  $\gamma$  of  $^{57}\text{Co}$  with a lifetime of  $1.5 \pm 4.0 - 0.07$  ps belongs to the i) category. The limits setted above seem therefore to be correct.

This rough classification is sometimes useful because it is not always possible to use DSAM on a self supporting target for lifetime measurements because of neighbouring peaks, while the observation of Doppler shift of a  $\gamma$  ray (or the non observation) is clear enough to set a upper limit (or a lower limit) to its lifetime.

4 - SPIN-PARITY ASSIGNMENTS : Spin-parity assignments have been deduced with more or less reliance using :

- the fact that in the fusion evaporation reactions,  $\gamma$  cascades usually proceed from higher to lower spin
- the angular distribution measurements (see Table 1 )
- the yield functions : increasing slope correspondsto increasing spin
- the lifetime measurements or estimations (see table 2 )
- the  $(\alpha, d)$  reaction results <sup>1,16</sup> : particularly 6 and 7 states strongly populated in this reaction are two-nucleon states and thus should have negative parity

The deduced level scheme is shown in Fig. 5. Table 3 presents the branching ratios of some levels in  $^{60}\text{Cu}$ .

The 287.2 keV level Auble <sup>7)</sup> adopts  $J^\pi = (1^+, 2^+)$ .  $J^\pi = 1^+$  must be rejected because this level is fed by a 270 keV  $\gamma$  ray (E2 transition) from the 557.5 keV level with  $J^\pi = 4^+$  (see below).

The 453.8 keV level. This level observed in the (<sup>3</sup>He, t) reaction <sup>8)</sup> with  $l = 4$  has positive parity ( $J^\pi = 3^+, 4^+, 5^+$ ) decays directly by a M1 transition to the ground state ( $J^\pi = 2^+$ ). Another weak branch (about 1%) of 167 keV  $\gamma$  is observed. So, we propose  $J^\pi = 3^+$  for this level.

The 557.5 keV level: The characteristics  $J^\pi = 4^+$  are confirmed by angular distributions of three  $\gamma$  rays issued from this level : 558 keV (E2), 270 keV (E2) and 104 keV (M1). E2 character are assigned by lifetime considerations as mentioned above.

The 781.0 keV level : Two  $\gamma$  are issued from this state . The (<sup>3</sup>He, t) reaction attributes  $3^+(4^+)$  to this level. We adopt  $3^+$  as the 781 keV  $\gamma$  ray is a M1/E2 transition ( $3^+ + 2^+$  g.s.).

The 1421.5 keV level : It can be identified to the 1432 keV state seen in the (<sup>3</sup>He, t) reaction. Angular distributions of the 967 keV  $\gamma$  ray can not rule out one of the proposed  $J^\pi = (3^+, 4^+)$ .

The 1603.6 keV level : It decays to the 557.5 keV level ( $J^\pi = 4^+$ ) by a M1/E2, 1046 keV  $\gamma$ -ray. Therefore this level has  $J^\pi = 5^+$ . It is strongly populated in the (<sup>3</sup>He, t) reaction with  $l = 6$  [ $J^\pi = 5^+, 6^+$ ] and in the ( $\alpha, d$ ) reaction which favours two-nucleon states. We conclude from the above arguments that it is probably the  $(\pi^2_{5/2} \nu^2_{5/2})_5^+$  state.

The 1778.9 keV level : This level is deexcited by two transitions : a 1325 keV E2 transition to the  $3^+$  state at 453.8 keV and a 1221 keV  $\gamma$  ray perturbed by the 1224 keV  $\gamma$ -ray in <sup>57</sup>Co. We propose  $J^\pi = 5^+$  to this level.

The 2026.6 keV level : A 1469 keV M1/E2 transition ( $A2 = -0.8, \delta = -1.7$ ) issued from this level feeds the  $J^\pi = 4^+$  level. So we propose  $J^\pi = 5^+$  to this level.

The 2197.2 keV level : This state is strongly populated in ( $\alpha$ , pny) and decays by a 1640 keV E2 transition ( $L = 2$  from angular distribution and  $\tau = 2$  ps) with an increasing yield function. So we propose that it is the  $6^+$  yrast level. (However we notice that the 1640 keV  $\gamma$  ray is not simple. It is in coincidence with another  $\approx 1640$  keV  $\gamma$  ray, but it can be estimated from coincidences measurements that the intensity of the second 1640 keV  $\gamma$ -ray represents only 10% of the total one).

The 2349.5 keV level : This level is deexcited by a 1792 keV  $\gamma$  ray. Spin-assignment is not possible because of an intense 1792 keV  $\gamma$ -ray in  $^{60}\text{Ni}$ .

The 2691.7 keV level : The 1088 keV  $\gamma$  ray has M1/E2 behaviour. We propose thus  $J^\pi = 6^+$  to this level.

The 2817.1 keV level : The angular distribution measurements give  $L=1$  to the 791 keV  $\gamma$  ray and we therefore suggest spin 6 to that state.

The 3066.5 keV level : This level is deexcited by a 2509 keV  $\gamma$  ray (see gates 558). Unfortunately, another  $\gamma$  ray with about the same energy belongs to  $^{60}\text{Ni}$  with comparable intensity so it is difficult to give any spin-assignment.

The 3155.5 keV level : This state decays through a 1552 keV  $L = 1$  transition. As the yield function is increasing we propose  $J = 6$  for this level. Furthermore, Lu et al <sup>1)</sup> have observed a strongly excited doublet at 3.29 MeV in the  $^{58}\text{Ni}(\alpha, d)$   $^{60}\text{Cu}$  reaction at  $E_\alpha = 26$  MeV and have shown that the two components of the doublet are located at 3.15 MeV and 3.33 MeV. So the 3155.5 keV level can be identified to the 3.15 MeV level seen in the ( $\alpha, d$ ) reaction. We then assign the characteristics  $J^\pi = 6^-$  to this state.

The 3190.8 keV level : The 1587 keV  $\gamma$  ray is an E2 transition ( $L = 2$  from angular distribution, and a lifetime of 3 ps rules out the M2 character). The yield function is increasing so we suggest  $7^+$ .

The 3354.5 keV level : An intense 1157 keV  $L = 1$  transition deexcites this level with an increasing yield function. This state can be identified to the 3.33 MeV level strongly excited in the ( $\alpha, d$ ) reaction. So we propose  $J^\pi = 7^-$  (negative parity yrast state).



The 3772.0 keV level : This state is deexcited by two  $\gamma$  transitions with about the same intensity. The 617 keV  $\gamma$  ray has  $L = 1$  character while 417 keV  $\gamma$  ray has  $A_2 = 0.26$  compatible with a  $J \rightarrow J$  transition. We propose thus  $7^-$  and negative parity since this level is strongly excited in the  $(\alpha, d)$  reaction <sup>1,16</sup>.

The 4520.8 keV level : Two perturbed  $\gamma$  rays deexcite this state so no spin can be assigned.

The 51881.1 keV level : Two  $L = 2$  transitions are issued from this level. E2 character is assigned to the 1834 keV  $\gamma$ -ray because the lifetime is 2 ps. The rapidly increasing yield function favours  $9^-$  assignment.

Remarks : The  $(\pi g_{9/2} \vee g_{9/2}) g^+$  level at 5.99 MeV is not sufficiently populated to make possible the observation of its  $\gamma$  decay.

In order to try to observe the  $\gamma$  decay of this state, the  $^{58}\text{Ni}(\alpha, d\gamma)^{60}\text{Cu}$  reaction at  $E_\alpha = 50$  MeV was performed. The deuterons were detected and identified using a two Si telescope ( $\Delta E = 1500 \mu$  and  $E = 5$  mm) located at  $\theta = 35^\circ$  with respect to the beam direction. The obtained deuteron spectrum was similar to that of Lu et al <sup>1)</sup>. However  $d-\gamma$  coincidences with the  $9^+$  peak did not allow us to determine directly the  $\gamma$  decay of  $9^+$  state because of its low cross-section.

## 6. DISCUSSION

In first approximation, the  $^{60}\text{Cu}$  can be regarded as a  $^{56}\text{Ni}$  inert core plus a proton and 3 neutrons in other active shells. If we consider, as in the calculations of Koops et al <sup>17)</sup> and Wang et al <sup>18)</sup>, only  $2p_{3/2}$ ,  $2p_{1/2}$  and  $1 f_{5/2}$  shells, the highest allowed spin is  $8^+$ . To explain negative parity states or positive parity states  $\geq 9^+$ , it is necessary to introduce the  $g_{9/2}$  shell ( $\sigma r$ ) and to break the  $^{56}\text{Ni}$  core). Excitation energies of some high-spin levels in  $^{60}\text{Cu}$  with  $J^\pi = 5^+, 6^+, 7^+$  determined in this experience can be compared to those calculated by Koops et al <sup>17)</sup> (see table 4). The agreement for the first states is good with MSDI or ASDI formalisms.

The level scheme of  $^{60}\text{Cu}$  is quite similar to that of  $^{62}\text{Cu}$  (Ref.4). The 3.155 MeV state  $J^\pi = 6^-$  decays by E1 transition to a  $5^+$  state which has the main configuration  $\pi f_{5/2}^+ \nu f_{5/2}^+$ . This behaviour is different from that of  $^{64}\text{Cu}$  (Ref.4) and  $^{66}\text{Cu}$  (Ref. 19,20) where the  $6^-$  level is isomeric and decays to a  $J^\pi = 4^+$  state through a M2 transition.

This phenomenon may be understood simply in the frame-work of our crude shell model <sup>3)</sup> for two-nucleon states. Indeed, the addition rule predicts the excitation energy of  $5^+$  state in odd-odd coppers between 1 and 1.3 MeV while the excitation energy of  $6^-$  states varies quickly from 1 MeV for  $^{66}\text{Cu}$  to 3 MeV for  $^{60}\text{Cu}$ . In the case of  $^{64}\text{Cu}$  and  $^{66}\text{Cu}$ , the  $5^+$  state may be very near by the  $6^-$  level so it may explain why the transition  $6^- \rightarrow 5^+$  state is not seen. (In  $^{64}\text{Cu}$ , the level at 1.59 MeV may be double and one member of the doublet is the  $6^-$  state, the other may be the  $5^+$  state seen in (d, $\alpha$ ) reaction <sup>20</sup>). On the contrary, in  $^{62}\text{Cu}$  and  $^{60}\text{Cu}$ , the  $6^-$  state lies well above the  $5^+$  state and we observe an intense  $6^- \rightarrow 5^+$  E1 transition.

The  $6^-$  level is very much populated through the ( $\alpha$ ,pn $\gamma$ ) reaction in all the studied odd-odd copper ( $^{60}\text{Cu}$ ,  $^{62}\text{Cu}$ ,  $^{64}\text{Cu}$ ,  $^{66}\text{Cu}$ ). The  $9^+$  state is much less feeded. In  $^{62}\text{Cu}$  and  $^{64}\text{Cu}$ , it decays by an E1 transition to the  $8^-$  state. Fig. 6 shows the striking correlation between the excitation energies of the  $6^-$  and  $9^+$  states and the  $g_{9/2}$  single particle energies in odd-odd coppers. For  $^{64}\text{Cu}$  and  $^{66}\text{Cu}$ , the (d,p) reactions give the main configuration of  $6^-$  state as  $(\pi p_{3/2} \nu g_{9/2}) 6^-$  without any equivoque. For  $^{60}\text{Cu}$  and  $^{62}\text{Cu}$ , the other configuration  $(\pi g_{9/2} \nu p_{3/2})$  is also possible. In  $^{60}\text{Cu}$ , our addition rule predicts neighbouring energies for these two configurations  $(\pi p_{3/2} \nu g_{9/2}) 6^-$  at 3.062 MeV and  $(\pi g_{9/2} \nu p_{3/2}) 6^-$  at 3.042 MeV. Probably there is a mixing of these two configurations.

The confrontation of results from  $\gamma$  spectroscopy studies and transfer reactions is once more fruitful : the assignment of negative parity to the two observed  $6^-$  states is natural with regard to the selection rule of the ( $\alpha$ ,reaction) and the main configuration can be assigned. Table 5 presents our propositions for spin and configuration assignment for strongly excited states in the  $^{58}\text{Ni}(\alpha,d)$  reaction and the comparison with values deduced from our crude-shell model. As for the other Cu isotopes (and also for Zn, Ga and Ge isotopes) we point out the importance of the role of

the  $g_{9/2}$  shell to build high-spin states. It would be interesting that conventional shell-model calculations in this region of nuclide chart can include the  $g_{9/2}$  shell and afford in this way a deeper explanation of high-spin states.

REFERENCES

- 1) C.C. Lu, M.S. Zisman, B.G. Harvey, Phys. Rev. 186 (1969) 1086
- 2) R. Jahn, D.P. Stahel, G.J. Wozniak, R.J. de Meijer and J. Cerny, Phys. Rev. C 18 (1978) 9
- 3) Tsan Ung Chan, M. Agard, J.F. Bruandet and C. Morand, Phys. Rev. C 19 (1979) 244
- 4) Tsan Ung Chan, M. Agard, J.F. Bruandet, A. Giorni and J.P. Longueue, Nucl. Phys. A257 (1976) 413
- 5) Tsan Ung Chan, M. Agard, J.F. Bruandet, A. Giorni, F. Glasser, J.P. Longueue and C. Morand, Nucl. Phys. A293 (1977) 207.
- 6) Tsan Ung Chan, M. Agard, J.F. Bruandet, A. Dauchy, A. Giorni, F. Glasser, J.E. Koops and C. Morand, Conf. on the structure of lighter nuclei, Bvar, Croatia, Yugoslavia (1978)
- 7) R.L. Auble, Nucl. Data Sheets, 28 (1979) 103
- 8) W.R. Zimmerman, J.J. Kraushaar, M.J. Schneider, H. Rudolph, Nucl. Phys. A297 (1978) 263
- 9) G.H. Dulfer, B.O. ten Brink, T.J. Ketel, A.W.B. Kalshoven and H. Verheul, Z. Phys. 251 (1972) 416
- 10) L. Birstein, Ch. Droxy, A.A. Jaffe and Y. Zioni, Nucl. Phys. A97 (1967) 203
- 11) E.J. Hoffman, D.G. Sarantities, Phys. Rev. 181 (1969) 1597
- 12) T. Yamazaki, Nucl. Data A3 (1967) 1

- 13) C. Morand, J.F. Bruandet, A. Giorni and Tsan Ung Chan, *J. de Phys.* 38 (1977) 1319  
C. Morand, J.F. Bruandet, B. Chambon, A. Dauchy, D. Drain, A. Giorni and Tsan Ung Chan, *Nucl. Phys.* A313 (1979) 45
- 14) G. Moyat, B. Delaunay, J. Delaunay, J. Eberth, V. Zobel and L. Cleemann, *Nucl. Phys.* A318 (1979) 236
- 15) N. Bendjaballah, B. Delaunay, J. Delaunay and T. Nomura, *Nucl. Phys.* A280 (1977) 228
- 16) N.E. Sanderson, R.G. Summers Gill, T. Taylor and A. Khan, Annual Report, Birmingham 1976 (unpublished)
- 17) J.E. Koops and P.W. Glaudemans, *Z. Phys.* A280 (1977) 181
- 18) M.C. Wang, H.C. Chiang, S.T. Hsieh and E.K. Lin, *Nuovo Cimento*, 29A (1975) 49
- 19) R.L. Auble, *Nucl. Data Sheets* 16 (1975) 383
- 20) Y.S. Park and W.W. Daehnick, *Phys. Rev.* 180 (1969) 1082
- 21) Tsan Ung Chan, J.F. Bruandet, B. Chambon, A. Dauchy, D. Drain, A. Giorni, F. Glasser and C. Morand, International Conference on Nuclear Behaviour at high angular momentum, Strasbourg, 1980
- 22) R.L. Auble, *Nucl. Data Sheets*, 14 (1975) 155

TABLE 1  
Results of the angular distribution measurements in  $^{60}\text{Cu}$

SECTION 1

$E_\gamma$	$E_1 + E_f$	$I_\gamma$	$A_2 \pm \Delta A_2$	$A_4 \pm \Delta A_4$	$J_1 + J_2$	$\sigma$	$a_2^2 + a_4^2$	$\delta \pm \Delta\delta$	$\chi^2$	Multipolarity and remarks
62.3	62.3 + 0	14	0.016 ± 0.12	-0.16 ± 0.17	1 <sup>+</sup> + 2 <sup>+</sup>	0.55	0.58 0.38	-0.17 - 0.5	0.9	
103.7	557.5 + 453.8	50	-0.24 ± 0.05	0.0 ± 0.08	4 <sup>+</sup> + 3 <sup>+</sup>	1.82	0.55 0.49	-0.03 - 0.5 + 0.2	0.75	M1
166.6	453.8 + 287.2	1.2	-0.35 ± 0.14	0.12 ± 0.18	3 <sup>+</sup> + 2 <sup>+</sup>	1.53	0.49 0.38	-0.18 - 0.5 + 0.2	0.85	
224.9	287.2 + 62.3	23.7	-0.20 ± 0.01	0.06 ± 0.02	2 <sup>+</sup> + 1 <sup>+</sup>	1.17	0.43 0.21	0 - 0.2 + 0.1	3	M1
270.3	557.5 + 287.2	17.8	0.26 ± 0.02	-0.11 ± 0.03	4 <sup>+</sup> + 2 <sup>+</sup>	1.66	0.60 0.42	-0.07 - 0.1 + 0.1	0.74	E2
287.2	287.2 + 0	10.3	0.02 ± 0.03	0.04 ± 0.04	2 <sup>+</sup> + 2 <sup>+</sup>	1.2	0.42 0.19	0.17 - 0.1 + 0.2	1.27	
327.2	781.0 + 453.8	4	-0.03 ± 0.27	0.63 ± 0.26	3 <sup>+</sup> + 3 <sup>+</sup>					
417.5	3772.0 + 3354.5	5.9	0.27 ± 0.10	0.20 ± 0.13	7 <sup>-</sup> + 7 <sup>-</sup>	2.2	0.74 0.69	-0.46 - 0.3 + 0.5	1.5	
453.8	453.8 + 0	100	-0.39 ± 0.03	0.07 ± 0.04	3 <sup>+</sup> + 2 <sup>+</sup>	1.53	0.49 0.38	-0.2 - 0.4 + 0.2	1.6	M1
557.5	557.5 + 0	92.2	0.23 ± 0.01	-0.04 ± 0.01	4 <sup>+</sup> + 2 <sup>+</sup>	2.1	0.49 0.38	0 ± 0.07	0.75	E2
616.5	3772.0 + 3155.5	6.6	-0.34 ± 0.06	-0.01 ± 0.08	7 <sup>-</sup> + 6 <sup>-</sup>	1.79	0.80 0.77	-0.05 - 0.25 + 0.1	0.76	
781.0	781.0 + 0	5.	-1.09 ± 0.12	0.17 ± 0.14	3 <sup>+</sup> + 2 <sup>+</sup>	0.7	10.88 0.48	-0.7 - 1 + 0.5	0.8	M1/E2
790.5	2817.1 + 2026.6	8.2	-0.32 ± 0.4	-0.04 ± 0.28	(6) + 5 <sup>+</sup>	1.5	0.84 0.80	-0.00 - 0.6 + 0.1	0.8	
967.7	1424.5 + 453.8	5			3 <sup>+</sup> (4 <sup>+</sup> ) + 3 <sup>+</sup>					perturbed by other lines
1046.1	1603.6 + 557.5	42.8	-0.95 ± 0.01	0.13 ± 0.01	5 <sup>+</sup> + 4 <sup>+</sup>	1.52	0.77 0.64	-0.9 0.1	0.79	M1/E2
1088.1	2691.7 + 1603.6	6.7	-1.57 ± 0.38	0.0 ± 0.22	6 <sup>+</sup> + 5 <sup>+</sup>	1.50	0.84 0.72	-1.2 - 0.5 + 0.5	5.	M1/E2
1157.3	3354.5 + 2197.2	30.4	-0.29 ± 0.04	0.17 ± 0.05	7 <sup>-</sup> + 6 <sup>+</sup>	2.06	0.77 0.74	-0.03 - 0.2 + 0.1	2.8	
1166.3	4520.8 + 3354.5									perturbed by $\gamma$ in $^{60}\text{Ni}$
1221.4	1778.9 + 557.5				5 <sup>+</sup> + 4 <sup>+</sup>					perturbed by $\gamma$ in $^{57}\text{Co}$
1325.1	1778.9 + 453.8	10.7	-0.50 ± 0.04	-0.09 ± 0.06	5 <sup>+</sup> + 3 <sup>+</sup>	1.2	0.86 0.71	-0.09 - 0.2 + 0.2	0.8	
1365.3	4520.8 + 3155.5									perturbed by $\gamma$ in $^{61}\text{Cu}$ and $^{59}\text{Ni}$
1416.1	5188.1 + 3772.0	3.8	0.09 ± 0.12	0.31 ± 0.20	9 <sup>-</sup> + 7 <sup>-</sup>	2.18	0.84 0.80	-0.18 ± 0.2	0.90	
1469.1	2026.6 + 557.5	14.8	-0.80 ± 0.09	0.20 ± 0.11	5 <sup>+</sup> + 4 <sup>+</sup>	1.45	0.79 0.60	-1.7 - 0.5 + 0.8	0.8	M1/E2
1551.9	3155.5 + 1603.6	16	-0.42 ± 0.04	0.19 ± 0.06	6 <sup>+</sup> + 5 <sup>+</sup>	1.8	0.77 0.73	-0.1 - 0.4 + 0.2	2.4	E1
1581.2	3100.8 + 1603.6	7.7	0.31 ± 0.10	0.22 ± 0.12	7 <sup>+</sup> + 5 <sup>+</sup>	2.5	0.67 0.62	-0.03 - 0.3 + 0.2	2.3	E2

477.9	3772.0 + 3354.5	5.9	0.12 ± 0.10	0.20 ± 0.15	7 <sup>+</sup> + 7 <sup>-</sup>	2.2	0.74	0.69	- 0.46	+ 0.5	1.5	
453.8	453.8 + 0	100	-0.39 ± 0.03	0.07 ± 0.04	3 <sup>+</sup> + 2 <sup>+</sup>	1.53	0.49	0.38	- 0.2	- 0.4	1.6	M1
557.5	557.5 + 0	92.2	0.23 ± 0.01	-0.04 ± 0.01	4 <sup>+</sup> + 2 <sup>+</sup>	2.1	0.49	0.38	0	± 0.07	0.75	E2
616.5	3772.0 + 3155.5	6.6	-0.34 ± 0.06	-0.01 ± 0.08	7 <sup>-</sup> + 6 <sup>-</sup>	1.79	0.80	0.77	- 0.05	- 0.25	0.76	
781.0	781.0 + 0	5.	-1.09 ± 0.12	0.17 ± 0.14	3 <sup>+</sup> + 2 <sup>+</sup>	0.7	10.88	0.48	- 0.7	+ 0.1	0.8	M1/E2
790.5	2817.1 + 2026.6	8.2	-0.32 ± 0.4	-0.04 ± 0.28	(6) + 5 <sup>+</sup>	1.5	0.84	0.80	- 0.00	+ 0.5	0.8	
967.7	1424.5 + 453.8	5			3 <sup>+</sup> (4 <sup>+</sup> ) + 3 <sup>+</sup>				- 0.00	+ 0.1	0.8	perturbed by other lines
1046.1	1603.6 + 557.5	42.8	-0.95 ± 0.01	0.13 ± 0.01	5 <sup>+</sup> + 4 <sup>+</sup>	1.52	0.77	0.64	- 0.9	0.1	0.79	M1/E2
1088.1	2691.7 + 1603.6	6.7	-1.57 ± 0.38	0.0 ± 0.22	6 <sup>+</sup> + 5 <sup>+</sup>	1.50	0.84	0.72	- 1.2	- 0.5	5.	M1/E2
1157.3	3354.5 + 2197.2	30.4	-0.29 ± 0.04	0.17 ± 0.05	7 <sup>-</sup> + 6 <sup>+</sup>	2.06	0.77	0.74	- 0.03	+ 0.2	2.8	
1166.3	4520.8 + 3354.5									+ 0.1		
1221.4	1778.9 + 557.5				5 <sup>+</sup> + 4 <sup>+</sup>							perturbed by γ in <sup>60</sup> Ni
1325.1	1778.9 + 453.8	10.7	-0.50 ± 0.04	-0.09 ± 0.06	5 <sup>+</sup> + 3 <sup>+</sup>	1.2	0.86	0.71	- 0.09	+ 0.2	0.8	perturbed by γ in <sup>57</sup> Co
1365.3	4520.8 + 3155.5											perturbed by γ in <sup>61</sup> Cu and <sup>59</sup> Ni
1416.1	5188.1 + 3772.0	3.8	0.09 ± 0.12	0.31 ± 0.20	9 <sup>-</sup> + 7 <sup>-</sup>	2.18	0.84	0.80	- 0.18	± 0.2	0.90	
1469.1	2026.6 + 557.5	14.8	-0.80 ± 0.09	0.20 ± 0.11	5 <sup>+</sup> + 4 <sup>+</sup>	1.45	0.79	0.60	- 1.7	- 0.5	0.8	M1/E2
1551.9	3155.5 + 1603.6	16	-0.42 ± 0.04	0.19 ± 0.06	6 <sup>-</sup> + 5 <sup>+</sup>	1.8	0.77	0.73	- 0.1	+ 0.8	2.4	E1
1587.2	3190.8 + 1603.6	7.7	0.31 ± 0.10	0.22 ± 0.12	7 <sup>+</sup> + 5 <sup>+</sup>	2.5	0.67	0.62	- 0.03	- 0.4	2.3	E2
1639.7	2197.2 + 557.5	56.8	0.33 ± 0.06	-0.23 ± 0.11	6 <sup>+</sup> + 4 <sup>+</sup>	1.45	0.85	0.76	0	+ 0.2	0.98	E2
1792.0	2349.5 + 557.5											perturbed by γ in <sup>60</sup> Ni
1833.6	5188.1 + 3354.5	3.2	0.22 ± 0.07	-0.06 ± 0.11	9 <sup>-</sup> + 7 <sup>-</sup>	2.75	0.75	0.71	- 0.14	- 0.1	0.98	E2
2509.0	3066.5 + 557.5				(5) + 4 <sup>+</sup>					+ 0.2		perturbed by γ in <sup>60</sup> Ni

$E_\gamma$  transition decays from  $E_1$  state ( $J^\pi = J_1$ ) to  $E_\Gamma$  state ( $J^\pi = J_\Gamma$ ).  $A_2$  and  $A_4$  are coefficients of Legendre polynomials  $I(\theta) = I_0(1 + A_2 P_2(\cos \theta) + A_4 P_4(\cos \theta))$  with  $I_0(453.8) = 100$ . The energies are in keV with a precision of 0.2 keV. The alignment parameter  $a_2$  is computed using a Gaussian substates distribution of width  $\sigma$  with formula and notations of Yamazaki 12).

TABLE 2

Lifetime measurements of levels in  $^{60}\text{Cu}$ .

$E_x$	$J^\pi$	$E_y$	$\theta_1^\circ$	$\tau_1$	$\tau_j$	$ M ^2$ in W.U.			$A(\tau=0)$	B	$\tau_1$	C	$\tau_2$	D	$\tau_3$	E	$\tau_4$
						E1	M1	E2									
454	$3^+$	454	25 160 40 150	>5 >5 >5 >5	>5	<0.07			0.32	0.18	20	0.25	1	0.25	50	0	
558	$4^+$	558	25 161 40 150	>8 >8 >8 >8	>8	<75			0.24	0.25	30	0.18	20	0.15	1.5	0.18	15
1604	$5^+$	1046	25	>4	>4	<4.10 <sup>-3</sup> <5			0.41	0.18	3	0.14	20	0.12	10	0.15	8
2198	$6^+$	1640	25 160	1.4 3.9	2 <sup>+3</sup> -1	2.5			0.45	0	0	0	0.38	20	0.17	10	
3156	$6^-$	1552	25 160	5 >5	5 <sup>+20</sup> -4	3.10 <sup>-5</sup>			0.44	0	0	0	0.24	10	0.32	1.5	
3191	$6^+$	1587	160	3	3 <sup>+20</sup> -4	2			1								
3356	$7^-$	1157	160	>5	>5	<8.10 <sup>-5</sup>			0.70	0	0	0	0.14	20	0.06	1.5	
3373	$7^-$	417	25 160	>5 >5	>5	<0.09			0.70	0.3	1.5						
5188	$9^-$	1834	25 160	1.5 3	2 <sup>+5</sup> -1	0.7			1								

The  $\gamma$ -ray with energy  $E_y$  decays from a level at  $E_x$  energy excitation with  $J^\pi$  characteristics.  $\tau_1$  is measured at the angle  $\theta_1$ .  $\tau_j$  is the final adopted value. The following columns precise quantities used to describe the feeding of the level (see explanations in Ref. 13). The energies are given in keV and the lifetimes in ps. The  $\theta = 25^\circ$  and  $160^\circ$  spectra have been got with a large volume GeLi with a 2.5 keV resolution at  $E_y = 1$  MeV, while  $\theta = 40^\circ$  and  $150^\circ$  spectra have been obtained using a smaller volume GeLi of better resolution (1.5 keV at  $E_y = 300$  keV) but smaller efficiency.



TABLE 3

Branching ratios of some levels in  $^{60}\text{Cu}$ 

LEVELS	$J^{\pi}$	$E_i \rightarrow E_f$	$E_{\gamma}$	BRANCHING RATIOS %
287	$2^{+}$	287 $\rightarrow$ 0	287	$30 \pm 3$
		287 $\rightarrow$ 62	225	$70 \pm 3$
454	$3^{+}$	454 $\rightarrow$ 0	454	$99 \pm 1$
		454 $\rightarrow$ 287	167	$1 \pm 1$
558	$4^{+}$	558 $\rightarrow$ 0	558	$58 \pm 4$
		558 $\rightarrow$ 287	270	$11 \pm 1$
		558 $\rightarrow$ 454	104	$31 \pm 3$
781	$3^{+}$	781 $\rightarrow$ 0	781	$55 \pm 10$
		781 $\rightarrow$ 454	327	$45 \pm 10$
3772	$7^{-}$	3772 $\rightarrow$ 3155	617	$53 \pm 10$
		3772 $\rightarrow$ 3355	417	$47 \pm 10$
5188	$9^{-}$	5188 $\rightarrow$ 3772	1416	$54 \pm 10$
		5188 $\rightarrow$ 3355	1834	$46 \pm 10$

TABLE 4

17)  
Comparison between calculated and observed excitation  
energies of first  $5^+$   $6^+$   $7^+$  levels in  $^{60}\text{Cu}$

$J^\pi$	M S D I	A S D I	Exp
$5^+$	1.76	1.69	1.604
	2.30	2.06	1.779 a)
$6^+$	2.40	2.03	2.198
	3.01	3.09	2.691 b)
$7^+$	3.27	3.01	3.191
	3.51	3.55	?

a) This level may have  $(\pi f_{7/2}^{-1} \nu f_{5/2})_{5^+}$  configuration. The level calculated by Koops et al may then be the 2.027 keV level.

b) This level may have  $(\pi f_{7/2}^{-1} \nu f_{5/2})_{6^+}$  configuration.

TABLE 5

Propositions for spin and configuration assignment for strongly excited states in the  $^{58}\text{Ni}(\alpha, d)^{60}\text{Cu}$  reaction - Comparison with the energies from crude shell model.

Energies (in MeV) of strongly excited states in $(\alpha, d)$	Energies (in MeV) of corresponding states in $(\alpha, p, \gamma)$	Proposed character and configuration	Calculated energy by crude shell model
1.63	1.604	$(\pi f_{5/2} \nu f_{5/2}) 5^+$	1.253
3.15	3.156	$\left\{ \begin{array}{l} (\pi p_{3/2} \nu g_{9/2}) 6^- \\ (\pi g_{9/2} \nu p_{3/2}) 6^- \end{array} \right.$	$\left\{ \begin{array}{l} 3.062 \\ 3.042 \end{array} \right.$
3.35	3.356	$(\pi g_{9/2} \nu f_{5/2}) 7^-$	3.381
3.73	3.773	$(\pi f_{5/2} \nu g_{9/2}) 7^-$	3.976
5.99	?	$(\pi g_{9/2} \nu g_{9/2}) 9^+$	6.104

FIGURE CAPTIONS

- 1) Single spectra of the  $^{58}\text{Ni} + \alpha$  reaction at  $E_{\alpha} = 32 \text{ MeV}$
- 2) Relative yield functions of some  $\gamma$  rays in  $^{60}\text{Cu}$
- 3) Selected spectra in coincidence with events in the indicated regions and with subtracted background.
- 4) Prompt spectra of the  $^{58}\text{Ni} + \alpha$  reaction obtained with a  $^{58}\text{Ni}$  target on Bi backing at  $\theta = 40^{\circ}, 90^{\circ}$  and  $160^{\circ}$ . The behaviour of "long lifetime  $\gamma$ " ( $\tau > 1 \text{ ps}$ ) for example 1046 keV, 1084 keV, 1157 keV is quite different from that of "short lifetime  $\gamma$ " ( $\tau < 2 \text{ ps}$ ) for example 1224 keV, 1640 keV, 1758 keV.
- 5) Decay scheme of  $^{60}\text{Cu}$  as a result of the present measurements.
- 6) Experimental energy of the  $J^{\pi} = 6^{-}$  and  $9^{+}$  states in odd-odd Cu isotopes as a function of the sum of two single particle energies. Data for  $^{66}\text{Cu}$  and  $^{68}\text{Cu}$  are from Ref. 19, 21, 22.

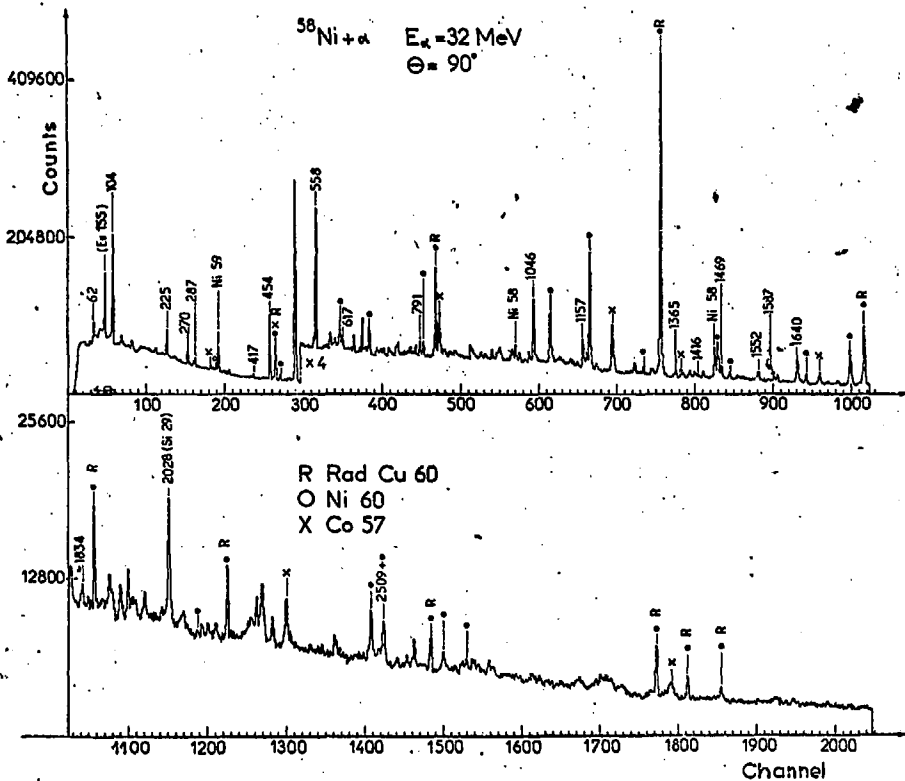


Fig. 1

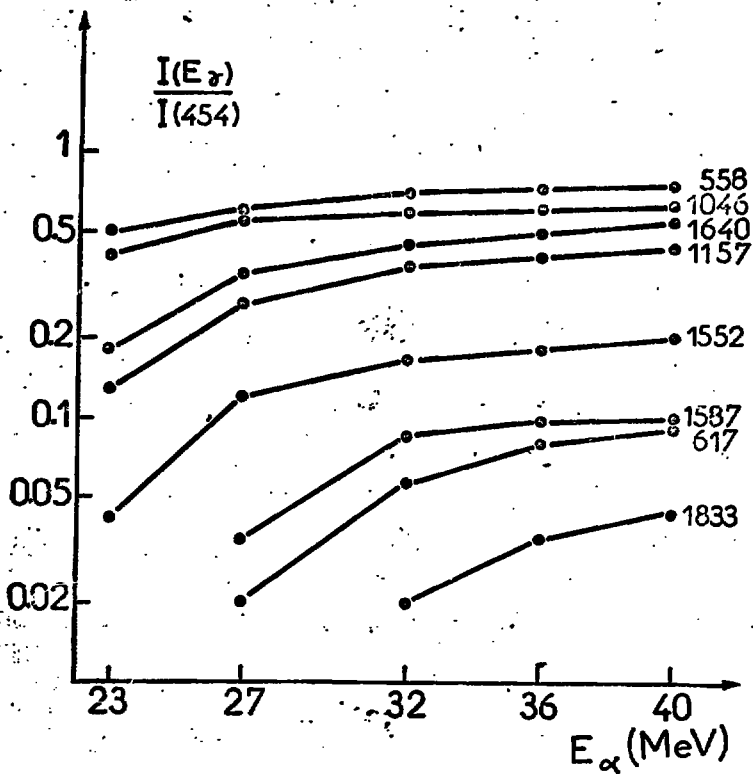


Fig. 2

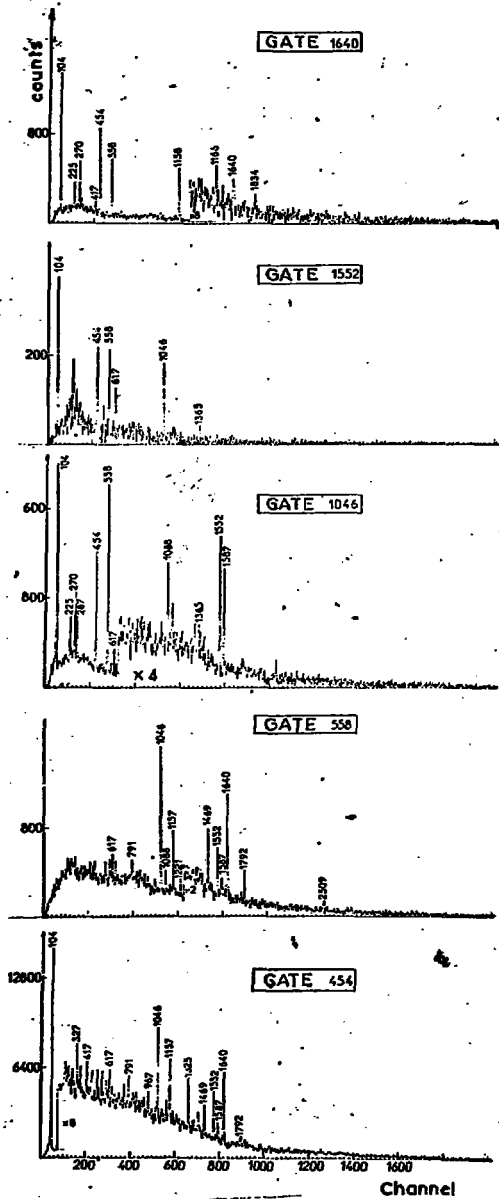


Fig. 3

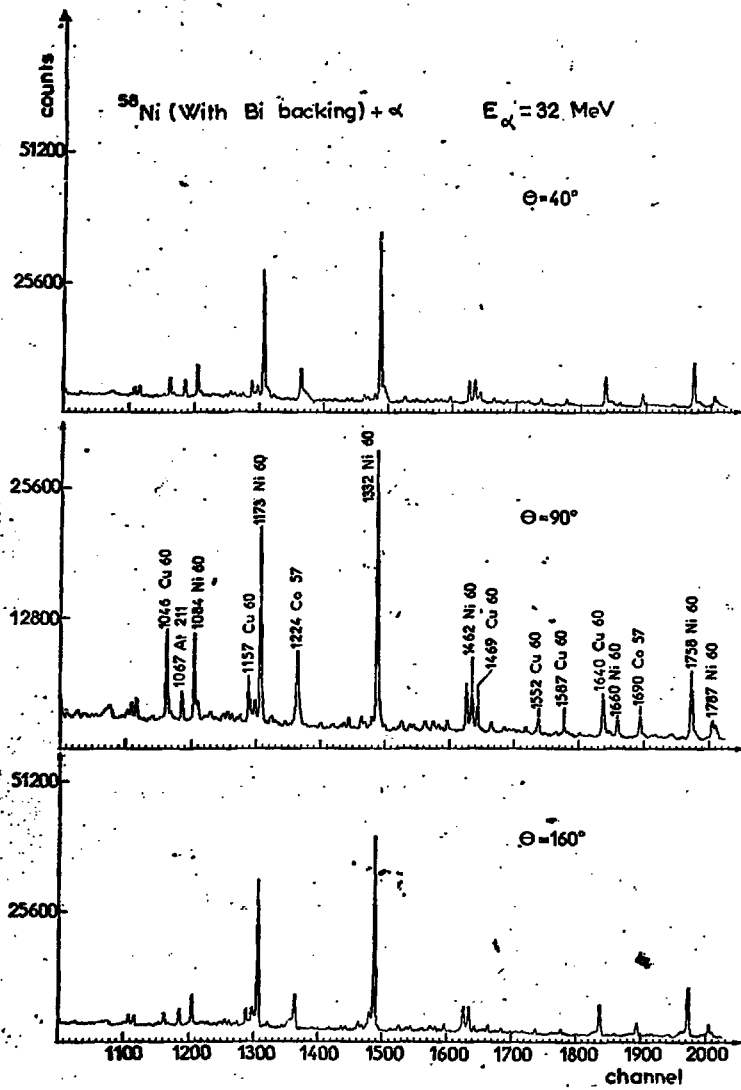
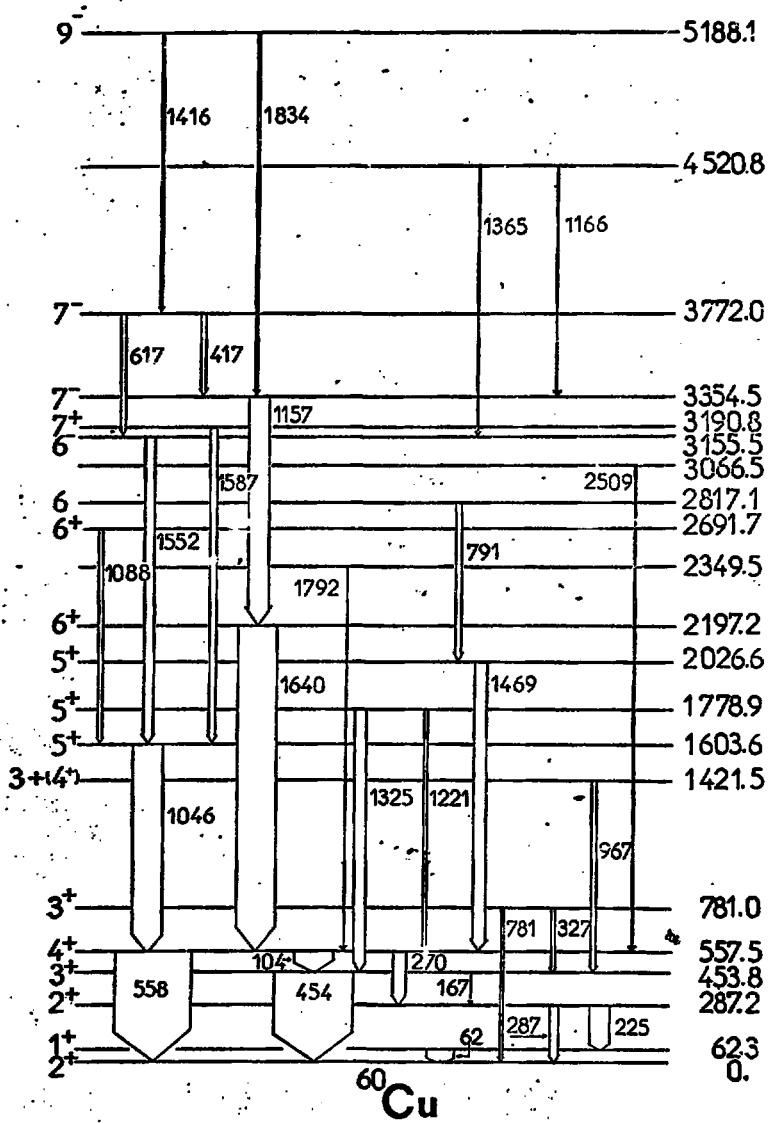


Fig. 4





$^{60}\text{Cu}$

Fig. 5

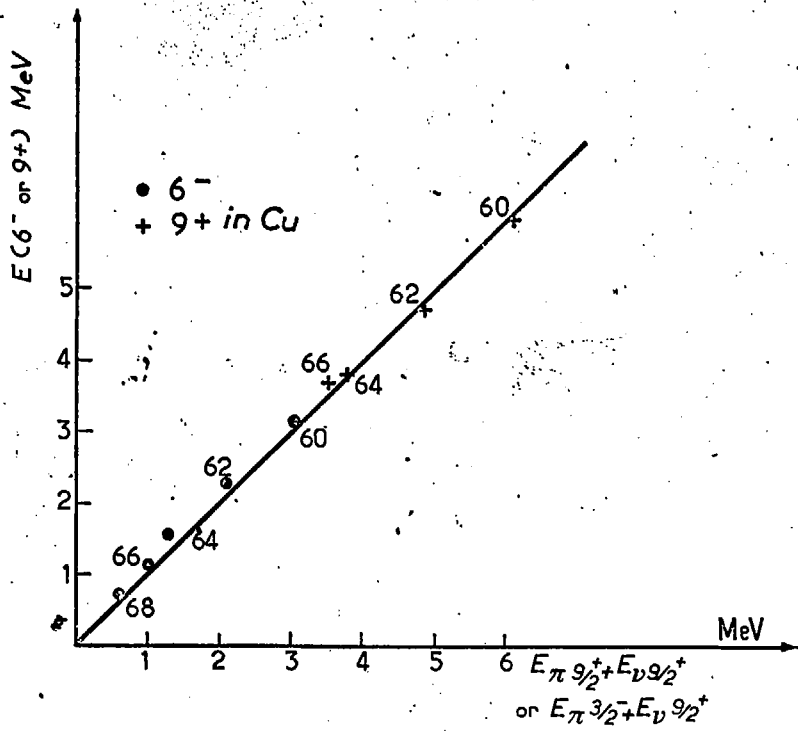


Fig. 6